Biosensors and Bioelectronics 147 (2020) 111787

Contents lists available at ScienceDirect

Biosensors and Bioelectronics

journal homepage: http://www.elsevier.com/locate/bios

2D magnetic MoS_2–Fe_3O_4 hybrid nanostructures for ultrasensitive exosome detection in GMR sensor

Feng Zhu [a,1], Dan Li [b,1], Qinfeng Ding [c], Chong Lei [a], Lizhu Ren [d], Xianguang Ding [e,**], Xuecheng Sun [a,*]

[a] Key Laboratory of Thin Film and Microfabrication (Ministry of Education), Department of Micro-Nano Electronics, School of Electronic Information and Electrical Engineering, Shanghai Jiao Tong University, Dongchuan Road 800, Shanghai, 200240, China
[b] Department of Dermatology, Nanjing Drum Tower Hospital, The Affiliated Hospital of Nanjing University Medical School, Nanjing, 210008, China
[c] Center of Craniofacial Orthodontics, Department of Oral and Craniomaxillofacial Surgery, Ninth People's Hospital, Shanghai Jiaotong University School of Medicine, Shanghai Key Laboratory of Stomatology & Shanghai Research Institute of Stomatology, National Clinical Research Center of Stomatology, Shanghai, 200011, China
[d] Department of Electrical & Computer Engineering, National University of Singapore, 117583, Singapore
[e] Nano-Bionics Division and i-LAB, Suzhou Institute of Nano-Tech and Nano-Bionics, Chinese Academy of Sciences, Suzhou, 215123, China

ARTICLE INFO

Keywords:
2D material
MoS_2
GMR
Exosome

ABSTRACT

Exosome released from cells plays an important role in intercellular communication and show great clinical potential in early cancer screening and prognosis. Herein, an ultrasensitive Giant Magnetoresistance (GMR) biosensor was developed for exosome detection, which was based on 2D MoS_2–Fe_3O_4 nanostructures (MOFE) as magnetic responsive probes for signal amplification. The MOFE can be readily synthesized with simple phase transfer method. Compared to pure Fe_3O_4 magnetic nanoparticles (MNPs), the layered MoS_2 function as a template for recruiting high loading density of MNPs as magnetic probes. After modified by aptamer, we discover that the 2D magnetic MOFE hybrid nanostructures enable both multidentate targeting and multi-magnetic particle-based signal amplification, increasing the magnetic sensor performance, especially in sensitivity and output signal. Moreover, the 2D magnetic nanocomposites afford high selectivity and excellent reproducibility with detection limit of 100 exosomes in GMR sensor. Results demonstrate that the magnetic strategy based on 2D structures introduced here provide a new dimension for exosome detection, which show great potential of engineering 2D magnetic nanobioprobes for GMR based liquid biopsy application.

1. Introduction

Exosome which generated by the outward blebbing of cellular membrane and thereby inherit cellular cargos such as mRNA, miRNA, DNA and membrane protein, has emerged as an attractive new biomarker these years in disease diagnostic and clinical management (Jeppesen et al., 2019; Van Niel et al., 2018). Compared to the traditional molecular evaluation, which remain the gold standard for tissue biopsies, exosome show great advantages of non-invasive and harvest limitless. Recent researches have shown that cancer derived exosome can be an effective alternative of cancer cells for cancer subtyping, stage and severity evaluating, as well as therapy monitoring (Contreras-Naranjo et al., 2017; Liu et al., 2018; Sheridan, 2016). On the other hand, as a new kind of biological object for bioassays, exosome show unique characteristics such as the small size of around 50–200 nm, which was large than proteins while much smaller than millimetre level of cells. These properties make exosome assay difficult. Especially, most conventional analytical strategies which were optimized for usual biological objects, show limitation in sensitivity and signal output for exosome research, which hinder the potential clinical application (Shao et al., 2018). Recent years, increasing attention and research have been drawn to address these challenges and develop exosome-optimized analytical platforms (Jiang et al., 2017; Liu et al., 2019; Shao et al., 2015; Wang et al., 2018; Zhang et al., 2019).

Giant magneto-resistive (GMR) sensor has attracted tremendous attention in biosensor due to the advantages such as high sensitivity, low

* Corresponding author.
** Corresponding author.
E-mail addresses: xgding2011@sinano.ac.cn (X. Ding), sunxc_2007@126.com (X. Sun).
[1] Those author contributed equally to this work.

https://doi.org/10.1016/j.bios.2019.111787
Received 28 August 2019; Received in revised form 2 October 2019; Accepted 13 October 2019
Available online 17 October 2019

cost, compatible with IC technology and suitable to integrate with microfluidic technology (Baselt et al., 1998). Currently, the idea of employing GMR sensor and superparamagnetic nanoparticle technology working as biosensor has received increasing research and development efforts (Rife et al., 2003). This technology has been applied for the bio target detection such as nucleic acids (Miller et al., 2001; Schotter et al., 2004; Xu et al., 2008), protein biomarkers (Choi et al., 2016; Graham et al., 2003), bacteria (Sun et al., 2016). Among the current detection method, The GMR biosensor signal was up to the magnetic label numbers that captured on the sensor surface, the current recognizing method was based molecular binding events (antigen-antibody interaction, ligand-receptor binding) , but one antibody/DNA can only capture one or two magnetic nanoparticle (Klein et al., 2019; Zhi et al., 2014). The relatively low recognizing efficiency and weak signal readout limit the GMR sensor detection performance and application in biology technology.

2D materials are fundamentally and technologically interesting because of their advantages of low cost, relative large surface area and layer-dependent properties, which promise their great potential in a variety applications such as catalysts, transistors, energy harvesting and biosensors (Chhowalla et al., 2013; Zhang et al., 2018). MoS_2, as an emerging new family of layered materials, provide new fundamental science and emergent applications due to their unique layered structures (Ding et al., 2019; Yin et al., 2011). Recent years, MoS_2-based nanostructures have been successfully used for the detection of metal ions, nucleic acids, proteins, and small molecules based on fluorescence or electronic sensor (Su et al. 2017a, 2017b; Sui et al., 2019; Wang et al., 2019; Zhu et al., 2013). On the other hand, 2D MoS_2 could also serve as unique template for assembling functional nanomaterials, thus providing an unprecedented handle for constructing multifunctional hybrid nanostructures with extra ordinal performance.

Here we demonstrate that 2D MoS_2 can be used a handle for facile synthesis of magnetically active MoS_2–Fe_3O_4 nanostructures (MOFE) via phase transfer strategy (Fig. 1a). The hybrid nanostructures show significant GMR sensitivity increase, which can be ascribed to the multivalent targeting and clustered Fe_3O_4 (MNP) induced signal amplification (Fig. 1b). Cancer cell-derived exosome was selected for this study. The aptamer modified 2D MOFE probes exhibited ultrasensitive detection capability of 100 exosome.

2. Materials and methods

2.1. Synthesis of 2D MoS_2–Fe_3O_4

Synthesis of 2D MoS_2. MoS_2 nanosheet was exfoliated from bulk MoS_2 powers in aqueous by surfactant sodium cholate. Typically, 250 mg of MoS_2 powders were dissolved in 50 mL of dH_2O containing 60 mg BSA. Then the mixture was sonicated for 48 h. After that the mixture solution was spin down at 2500 rpm for 15 min and the supernatant solution containing exfoliated 2D MoS_2 were collected. For purification, the collected MoS_2 was further centrifuged at 12,000 rpm at 30 min to remove free BSA. The Fe_3O_4 were synthesized according the typical solvothermal method. The corresponding 2D MoS_2–Fe_3O_4 were synthesized via phase transfer using MoS_2 as substrate and BSA on MoS_2 as chelating points. Typically, Hydrophobic Fe_3O_4 NPs were dispersed in 2 mL of hexane and then added into 5 mL of aqueous MoS_2 solution under vigorous stirring. The MoS_2–Fe_3O_4 with different loading amount of Fe_3O_4 can be readily obtained at different timepoints in aqueous solution. For example, MOFE with three different loading amounts of Fe_3O_4 were collected via the phase transfer strategy at 60 min, 90 min and 120 min, which were noted as MOFE-1, MOFE-2 and MOFE-3, separately. The obtained nanostructures were then washed and purified.

2.2. Surface modification of MoS_2–Fe_3O_4 nanostructures

Aptamer modification on 2D MoS_2–Fe_3O_4 nanostructures via the amino reacted with carboxyl group derived from BSA functionalized on MOFE surface. In brief, 50 mg MoS_2–Fe_3O_4 and amino modified aptamer were dispersed in 5 mL of Dimethyl Formamide (DMF). Then 10 μL of triethylamine and 10 mg of 1-ethyl-3-(3-dimethylaminopropyl)

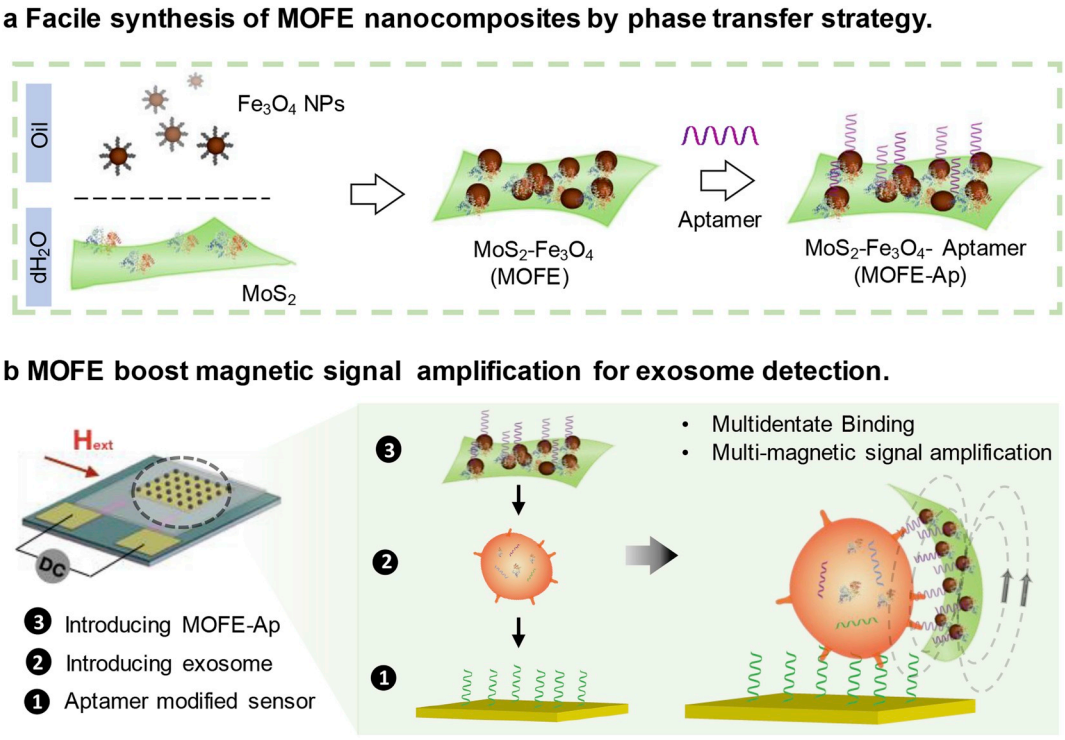

Fig. 1. a. Schematic illustration of the synthesis of MOFE nanostructure by phase transfer approach and the following-up aptamer functionalization. **b**. Schematic illustration of multivalent binding of MOFE nanostructure with a single exosome.

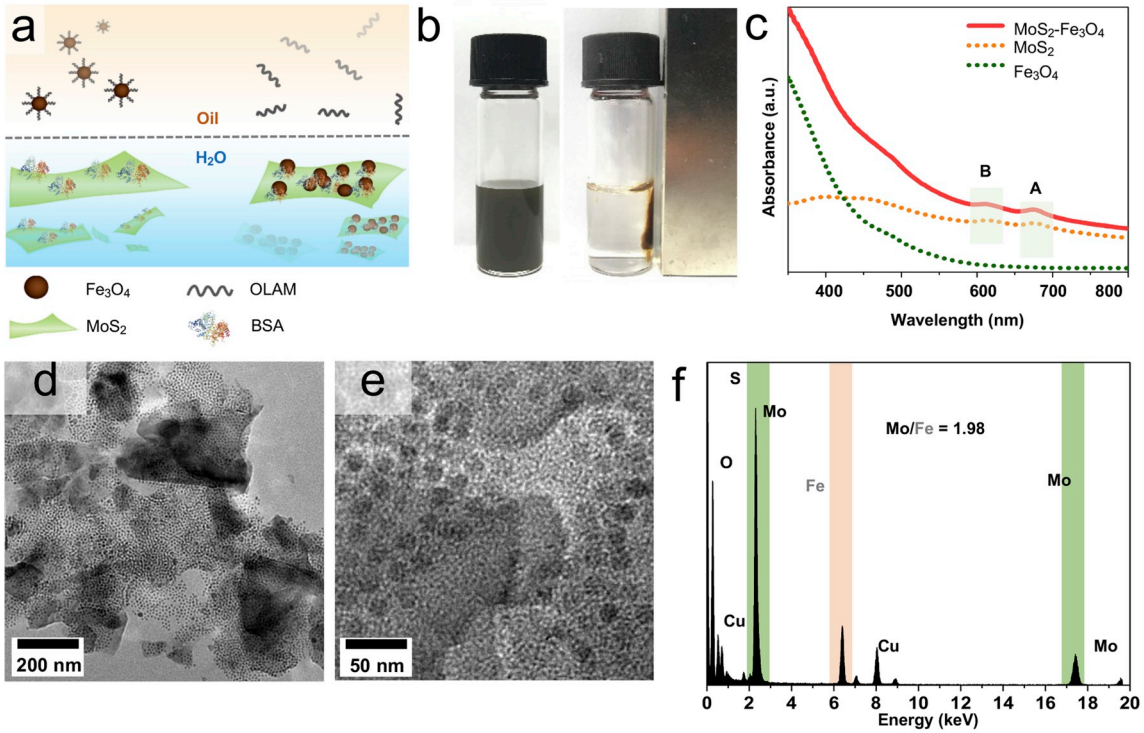

Fig. 2. **a**. Schematic illustration of the formation of MOFE nanocomposites by phase transfer approach. **b**. Photographs of an aqueous solution of MOFE nanostructures in the absence and presence of a magnet. c. UV–vis spectrum of MoS_2–Fe_3O_4, MoS_2 and Fe_3O_4. d, e and f. TEM, HRTEM images and EDS of the MoS_2–Fe_3O_4 nanostructures.

carbodiimide were introduced into the mixture solution subsequently. After stirring overnight at room temperature, aptamer modified MoS_2–Fe_3O_4 can been obtained by washing and centrifugation several times.

Corresponding aptamer sequence used: CD63 (CAC CCC ACC TCG CTC CCG TGA CAC TAA TGC TA) and EpCAM (CA CTA CAG AGG TTG CGT CTG TCC CAC GTT GTC ATG GGG GGT TGG CCT G).

2.3. GMR sensor fabrication

The GMR film structure detail was as follow:

Si/Ta(5 nm)/FeNi(3 nm)/IrMn(8 nm)/CoFe(2 nm)/Ru(1 nm)/CoFe(2 nm)/Cu(3 nm)/CoFe(1.5 nm)/FeNi(3 nm)/Ta(3 nm). The GMR film material was deposition on a silicon wafer by Multi-target magnetron sputtering. Mask alignment was used to pattern GMR stripes, ion milling was employed to transfer the pattern. After removed the photoresist, the GMR stripes were made. Cr/Cu (5nm/100 nm) layer was then deposited on the leads and pads pattern by sputtering system, after removed the photoresist, the Cr/Cu leads and pads were fabricated. SiO_2 (50 nm) was deposited on the sensors surface except leads and pads area. And a thickness (50 nm) Au was deposited on GMR strip area for bio-modification. A SU-8 micro-wall was fabricated on GMR sensor surface for bio-detection, the wall thickness was 500 μm. The single chip including 100 strips in serial connection with single strip of 500 μm × 5 μm electrical active area.

2.4. GMR surface functionalization

The GMR chip was firstly washed with 100% acetone, 100% methanol, and 100% DI water, dried by N_2. Then 20 μL of thiol modified aptamer dispersed in pure water was added into the strips area. After incubating at room temperature for 6 h, the free aptamer ligand was washed away.

2.5. GMR sensor testing system

The GMR sensor was test in direct current (DC) plane mode. The testing system include three parts: Helmholtz coil, Source meter 2450, GMR chip holder. The Helmholtz coil was employed for supplying the external magnetic field to excite GMR sensor, DC current power was implemented to control the magnetic field intensity. The sourcementer2450 was used for exciting and measuring the sensor voltage signal. The GMR chip holder for fixing the GMR sensor with a stable position for test.

3. Results and discussion

3.1. Designing and characterization of magnetic 2D MOFE composites

We employed phase transfer strategy to construct MOFE hybrid nanostructure. The MoS_2 nanosheet in water and MNPs in hexane were firstly prepared (Fig. S1). The abundant amino groups of BSA on MoS_2 can easily coordinate MNPs, enabling MNPs readily attached to MoS_2 surface from organic solvents through ligand exchange. The phase transfer process was illustrated in Fig. 2a. The magnetic properties of MOFE after collection was studied. In the presence of a magnet, the composites well dispersed in dH_2O can be easily isolated and purified (Fig. 2b). The ultraviolet and visible (UV–vis) spectrum of MOFE clusters were also checked (Fig. 2c). Compared with MNPs, two strong absorption bands at 666 nm and 605 nm occurred in MOFE curve, which arise from the typical electronic transitions in the band structure of exfoliated MoS_2, indicating the successful formation of MOFE hybrid structures. Typical transmission electron microscope (TEM) images of the as-synthesized MOFE nanocomposites show that the MoS_2 nanosheets exhibited an average size of around 100 nm, with large numbers of MNPs about 10 nm attached on 2D MoS_2 nanosheets (Fig. 2d and e). Furthermore, the corresponding EDS result show the presence of Mo, S and Fe elements (Fig. 2f), which was consistent with the TEM

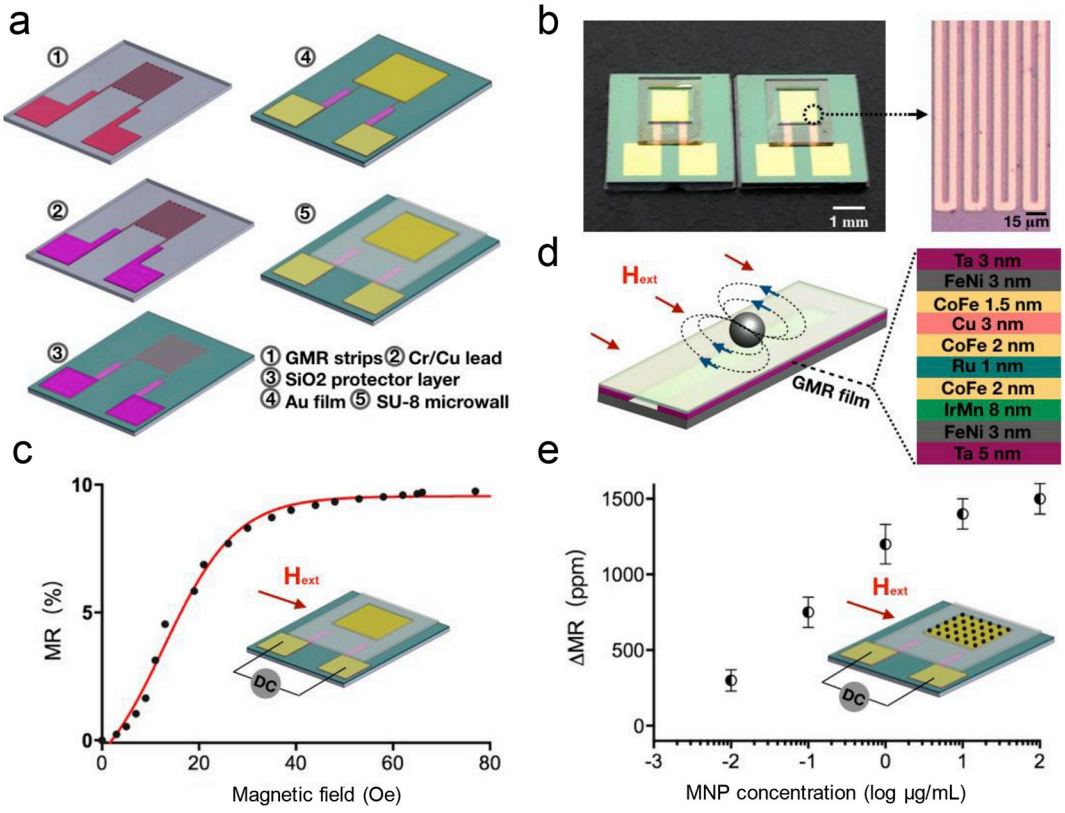

Fig. 3. **a**. Fabrication steps of GMR sensor. **b**. The fabricated GMR sensor and GMR strips. **c**. The basic performance of GMR sensor. **d**. Detection mode of magnetic nanoparticle detected by GMR sensor. **e**. MNP (10 nm) detection performance of GMR sensor.

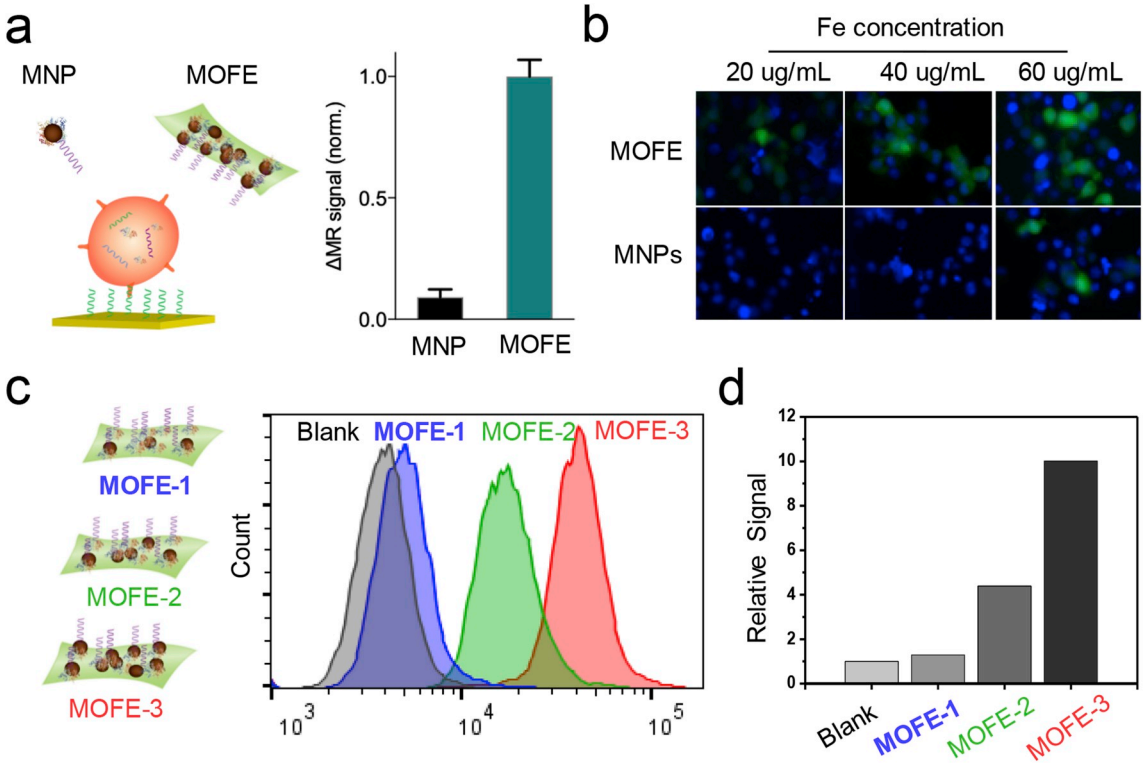

Fig. 4. **a**. MOFE boosting GMR signal for exosome detection. **b**. Fluorescence images of A431 cells treated with aptamer CD63 labelled MOFE and Fe_3O_4 nanostructures in the absence and presence of a magnet. **c**. Flow cytometric profiles of the A431 cells treated with MOFE-1, MOFE-2 and MOFE-3 after 1 h. **d**. Relative fluorescence intensity of the cells after treating with CD63 labelled MOFE nanostructures with different amounts of MNP.

observation. The XRD characterization of the hybrid MOFE nanostructures show typical MoS_2 (JCPDS: 24–0513) and Fe_3O_4 structures (JCPDS: 03–0862) (Fig. S2). Conclusively, these characterizations confirm the successful incorporation and strong anchor of MNPs onto MoS_2 nanosheets in the hybrid nanocomposites.

3.2. Magnetic nanoparticles detecting by GMR biosensor

The GMR sensor fabrication steps were shown in Fig. 3a, the fabricated GMR sensor was shown in Fig. 3b. GMR sensor basic performance was tested before detecting MNP as shown in Fig. 3c. The maximum MR was equal to 9.23%, the linearity ranges was from 5 Oe to 30 Oe with sensitivity 0.32%/Oe. The Magnetic nanoparticle detection mode was in shown in Fig. 3d. When MNP was captured on the GMR sensor surface, under the external magnetic field magnetized, the MNP can induce a weak magnetic field. The weak magnetic field was generally opposite to the DC external magnetic field. The location magnetic field can be changed by the weak magnetic field induced by MNP, and the GMR sensor can readout the magnetic flied change. So, the presence of MNP can be detected by GMR sensor.

10 nm magnetic nanoparticle (MNP) with different concentrations (0.01 μg/mL, 0.1 μg/mL, 1 μg/mL, 10 μg/mL, 100 μg/mL) were used for testing. According to GMR basic performance curve, magnetic field with 25 Oe was employed as the sensor exciting magnetic field. 5 μL magnetic nanoparticle solution was dropped in GMR sensor micro-wall, after dry in room temperature, it was tested. The output signal was defined as $\Delta MR = MR_{basic}\text{-}MR_{Sample}$, the MR_{basic} means the GMR sensor basic performance, the MR_{sample} means the GMR sensor performance with MNP sample. It can be seen from Fig. 3e, samples from 0.01 to 10 μg/mL sample could be clearly distinguished from each other, the so this GMR biosensor can be utilized in detecting biomarker. The repeatability eR was 0.98%, the detection time was about 10 s.

3.3. MOFE increase the detection sensitivity by boosting GMR signal

Next, we evaluated the detection sensitivity of the MOFE by employing MOFE-CD63 for targeting the exosome surface marker CD63. CD63 was selected here as it was highly expressed on most of the cell surface. The exosome derived from A431 cell lines were firstly captured on GMR sensor surface by immobilized aptamer. Upon stained by different probes, the GMR signal response was quite different (Fig. 4a). Negligible MR signal change was found for pure MNPs, whereas the 2D MoS_2-recruited MNP nanocomposites showed dramatically enhanced MR signal with the same Fe_3O_4 concentration. To explore how the detection sensitivity vary with the MNP states. FITC was used to label MNPs for clearly visualizing the targeting sensitivity by molecular imaging. For comparison, both MNPs and MOFE were subjected to label CD63 aptamer for targeting. Then A431 cells were incubated with MOFE or MNPs at 37 °C for 1 h and cell PL images were acquired on an inverted fluorescence microscope. Fig. 4b suggested that A431 cells treated with MOFE show much stronger PL than that treated with MNPs at various Fe concentrations ranging from 20 μg/mL to 60 μg/mL, indicating the superior targeting specificity of MOFE toward A431 cells than pure MNPs. In particular, MOFE could offer strong cell imaging signals at very low Fe concentration (20 μg/mL), which could not be achieved by MNPs even when reaching the two times of Fe amount.

To further confirm the dependence of targeting sensitivity on MoS_2, additional two classes of MOFE with different MNPs loading amount were prepared. The phase transfer strategy enable the loading density of MNP tunable by simply adjusting stirring time. As shown in Fig. S3. The UV–vis absorption spectra of MOFE obtained at different time points varied with prolonging mixing time. As stirring time prolong, weaker UV–Vis absorbance at the characteristic peak of MoS_2 was observed, together with increase of absolute absorbance, which suggested that more and more MNPs became anchored on 2D MoS_2 nanosheets. Three

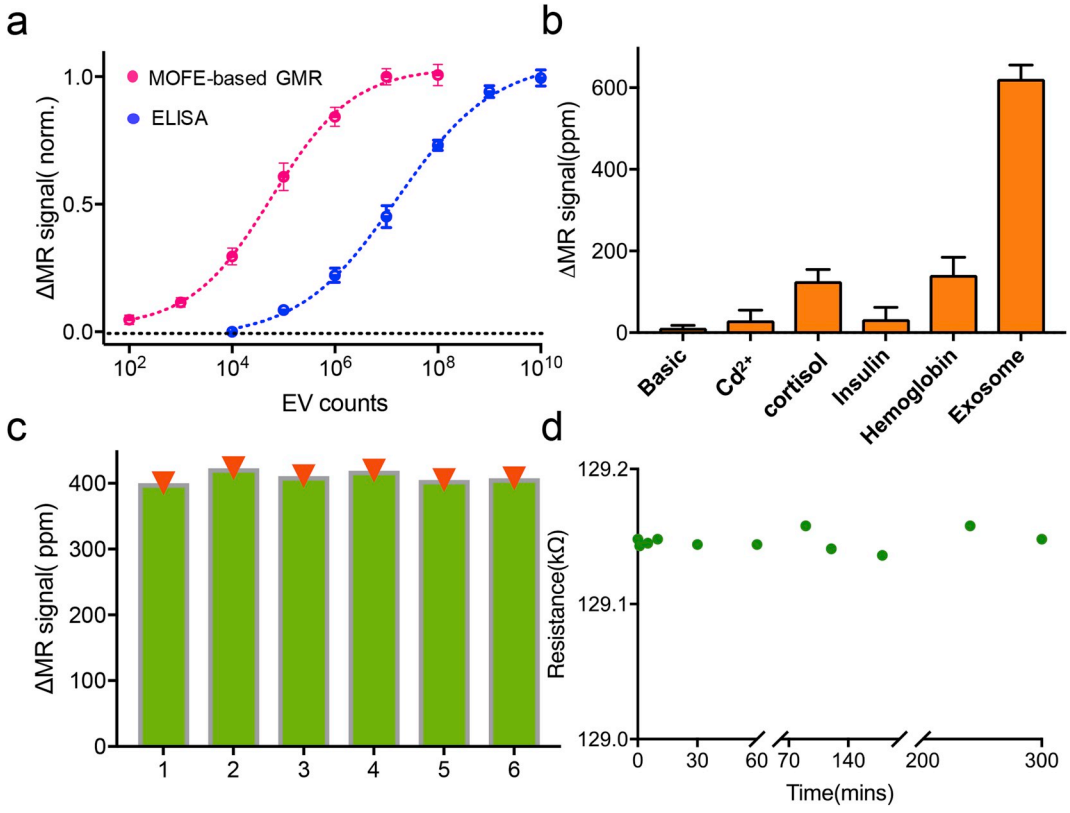

Fig. 5. **a**. Comparison of the detection sensitivities of MOFE-based GMR assay and golden standard ELISA for exosome detection. **b**. Selectivity of the CD63 labelled MOFE nanostructures-based sensor in the presence of Cd^{2+}, cortisol, insulin, haemoglobin and exosome. **c**. Reproducibility of the constructed MOFE-based GMR sensor. **d**. Stability of the GMR signal under the detection for 5 h.

classes of MOFE with different amounts of MNP loading amount were obtained via the phase transfer strategy, which were noted as MOFE-1, MOFE-2 and MOFE-3, related to the relative loading amount. Then the synthesized MOFE were applied to probe A431 cells. As shown in Fig. 4c, the flow cytometric profiling of cells treated with MOFE show significant signal increases following the increasement of MNP loading amount, in which MOFE-3 exhibited the highest fluorescence signal. The corresponding quantification of the flow cytometry was also conducted. A431 cells treated with MOFE-3 show stronger fluorescence than that treated by MOFE-2 and MOFE-1 (Fig. 4d), in which MOFE-3 impart 10 times, MOFE-2 impart 4.4 times, and MOFE-1 impart 1.3 times of the control signal.

Collectively, with MOFE as probe, the detection sensitivity of GMR sensor can be greatly enhanced. This sensitivity enhancement is most likely due to the 2D layered structure of MoS_2 nanosheets, which recruit abundant of localized MNPs for signal amplification and are more favourable for multidentate binding with biomarker.

3.4. Magnetic sensing of exosome

Next, the designed GMR combined with MOFE were further applied for analysing exosome samples. 10 μL of purified exosome sample from A431 cell culturing medium was dispersed in PBS and injected into the micro GMR chamber. After that the captured exosomes were incubated with MOFE, which were functionalized with aptamer against CD63. The resulting ΔMR signal show exosome amount dependent increase (Fig. 5a, Fig. S4). A highly correlation between MR signal change and exosome number which was independently determined by NTA was observed. It was worth to note that the MOFE-based biosensor established here show a large dynamic range spanning 5 orders of magnitude with the detection limit of around 100 exosomes, which outperform the commercialized chemiluminescence ELISA and is superior than most of the reported exosome sensors (Table 1). Importantly, this 2D magnetic material based magnetic assay is simple and background free, which can be finished within half an hour.

3.5. Specificity, reproducibility and stability of the MOFE magnetic sensor

To demonstrate the specificity of the MOFE-based GMR sensor, the GMR sensor was pre-immobilized with CD63 aptamers for capturing exosomes. After that same amount of exosomes were introduced into GMR biosensors chamber. In addition to functionalizing MOFE with CD63 aptamer for signal readout, three kinds of MOFE modified with nonspecific aptamers were also chosen (Cd ion, cortisol, insulin and haemoglobin). Fig. 5b show that the GMR signal show little change when nonspecific aptamers (Cd ion, cortisol, insulin and haemoglobin, respectively) functionalized MOFE were applied to exosomes treatment. The corresponding GMR value change were found to be 30.13 ppm, 126.16 ppm, 33.14 ppm, and 141.71 ppm, respectively. In contrast, the ΔMR was increased to be 621.29 ppm for exosomes treated with aptamer CD63 functionalized MOFE. These result suggested that aptamer modified MOFE can be used to specifically detect exosomes via GMR biosensor.

We next tested the specificity by changing biomarker. Cd ion, cortisol, insulin and haemoglobin and exosomes were selected as analysts and introduced into the aptamer CD63 functionalized GMR sensor. Then probe MOFE-CD63 was added into GMR chip for signal readout. For the nonspecific analysts, negligible MR signal changes were observed after the staining of MOFE-CD63 (Fig. S5). However, when exosomes were introduced in, the ΔMR value show significant increase, confirming the specificity of MOFE-based GMR sensor. Such excellent specificity would benefit MOFE-based analysis in complex biological sample.

The reproducibility of the MOFE-based GMR sensor was also studied through preparing six MOFE probes independently. The RSD was 8.7% for exosomes with concentration of 10^6/mL analysed (Fig. 5c), revealing the satisfying reproducibility of the MOFE-based immunosensor.

The stability of the biosensor was also investigated. As shown in Figs. 5d and 11 times of detection within 300 min caused no obvious change in the detected magneto-resistance change, demonstrating that the constructed MOFE-based biosensor possess excellent stability. The performance of MOFE-based GMR sensor was quite stable at pH value from 6 to 10 and show temperature tolerance from 20 °C to 40 °C (Fig. S6, Fig. S7).

3.6. Application of the constructed MOFE sensor in real samples

To demonstrate the clinical diagnostic potential, exosomes derived from A431 cell lines were mixed with 10% FSA to mimic real blood sample for clinical capability evaluation. After incubating the captured exosomes on GMR substrate with aptamer CD63 labelled MOFE for 30 min and washed the free MOFE away, the signal was measured by the GMR testing system. Fig. 6 show that the biosensor still have comparable MR signal in the artificial samples, suggesting the strong potential of MOFE for facilitating biomedical analysis applications (Fig. 6a). In order to verify their capability for the determination of exosome in real samples, the designed 2D magnetic probes were further applied to cancer diagnosis. We used native plasma samples directly to detect the exosomes. 10 μL of samples were dropped in the CD63 aptamer functionalized GMR micro-wall. After incubation for 1 h, EpCAM labelled MOFE were introduced to stain the captured exosomes. The initial screening with blood samples from 6 healthy volunteers and 3 ovarian cancer patients suggest that the EpCAM from exosomes might be potential marker for clinical indication (Fig. 6b). These preliminary results demonstrate that the potential of the constructed 2D magnetic material liquid biopsy application.

4. Conclusions

In summary, a simple, facile and low cost magnetic 2D MoS_2–Fe_3O_4 NPs have been developed for signal-amplified magnetic detection of liquid biomarkers. The magnetic sensitivity of 2D MoS_2–Fe_3O_4 NPs is significantly improved over single Fe_3O_4 NPs, allowing strong GMR signal could be achieved at very low probe concentration. More importantly, MoS_2–Fe_3O_4 could offer much higher exosome discrimination factor than pure MNPs, thus highlighting their potential for accurate and sensitive detection of liquid biomarker such as exosome. The reported 2D layered MoS_2–Fe_3O_4 composites pave the way for engineering 2D-magnetic based probes with enhanced GMR sensitivity for liquid biopsy. In this study, only CD63 and EpCAM on exosome surface were checked, which narrow its potential of clinical cancer identification. In the future, more exosomal protein markers should be involved and the specificity need be further justified. With these improvements, we further envision extending the clinical applications that if the 2D magnetic MoS_2–Fe_3O_4 based GMR sensor can differentiate the subtype

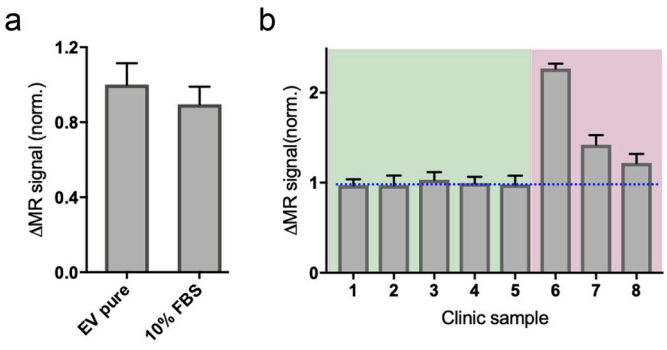

Fig. 6. **a**. GMR response to pure exosome and artificial serum after the staining of MOFE. **b**. EpCAM expression level of exosome in health (n = 5) and ovarian cancer patients (n = 3).

of ovarian cancers by profiling and combing different exosomal surface markers together once more patient numbers were involved.

Declaration of competing interest

The authors declare that they have no known competing financial interests or personal relationships that could have appeared to influence the work reported in this paper.

CRediT authorship contribution statement

Feng Zhu: Investigation, Methodology. **Dan Li:** Data curation. **Qinfeng Ding:** Formal analysis. **Chong Lei:** Funding acquisition, Software. **Lizhu Ren:** Formal analysis, Methodology. **Xianguang Ding:** Conceptualization, Writing - original draft. **Xuecheng Sun:** Conceptualization, Supervision, Writing - review & editing.

Acknowledgments

This work is supported by The National Natural Science Foundation of China (No.61273065, No.81901002), Support fund of Shanghai Jiao Tong University (AgriX2015005), Support fund of Joint research center for advanced aerospace technology of Shanghai Academy of Spaceflight Technology-Shanghai Jiao Tong University (USCAST2015-2), Support fund of aerospace technology (15GFZ-JJ02-05), Shanghai Sailing Program(No.19YF1425800), the Analytical and Testing Center in Shanghai Jiao Tong University, the Center for Advanced Electronic Materials and Devices in Shanghai Jiao Tong University.

Appendix A. Supplementary data

Supplementary data to this article can be found online at https://doi.org/10.1016/j.bios.2019.111787.

References

Baselt, D.R., Lee, G.U., Natesan, M., Metzger, S.W., Sheehan, P.E., Colton, R.J., 1998. A biosensor based on magnetoresistance technology. Biosens. Bioelectron. 13 (7–8), 731–739.

Chhowalla, M., Shin, H.S., Eda, G., Li, L.-J., Loh, K.P., Zhang, H., 2013. The chemistry of two-dimensional layered transition metal dichalcogenide nanosheets. Nat. Chem. 5 (4), 263.

Choi, J., Gani, A.W., Bechstein, D.J., Lee, J.-R., Utz, P.J., Wang, S.X., 2016. Portable, one-step, and rapid GMR biosensor platform with smartphone interface. Biosens. Bioelectron. 85, 1–7.

Contreras-Naranjo, J.C., Wu, H.-J., Ugaz, V.M., 2017. Microfluidics for exosome isolation and analysis: enabling liquid biopsy for personalized medicine. Lab Chip 17 (21), 3558–3577.

Ding, X., Peng, F., Zhou, J., Gong, W., Slaven, G., Loh, K.P., Lim, C.T., Leong, D.T., 2019. Defect engineered bioactive transition metals dichalcogenides quantum dots. Nat. Commun. 10 (1), 41.

Graham, D., Ferreira, H., Freitas, P., Cabral, J., 2003. High sensitivity detection of molecular recognition using magnetically labelled biomolecules and magnetoresistive sensors. Biosens. Bioelectron. 18 (4), 483–488.

Jeppesen, D.K., Fenix, A.M., Franklin, J.L., Higginbotham, J.N., Zhang, Q., Zimmerman, L.J., Liebler, D.C., Ping, J., Liu, Q., Evans, R., 2019. Reassessment of exosome composition. Cell 177 (2), 428–445 e418.

Jiang, Y., Shi, M., Liu, Y., Wan, S., Cui, C., Zhang, L., Tan, W., 2017. Aptamer/AuNP biosensor for colorimetric profiling of exosomal proteins. Angew. Chem. Int. Ed. 56 (39), 11916–11920.

Klein, T., Wang, W., Yu, L., Wu, K., Boylan, K.L., Vogel, R.I., Skubitz, A.P., Wang, J.-P., 2019. Development of a multiplexed giant magnetoresistive biosensor array prototype to quantify ovarian cancer biomarkers. Biosens. Bioelectron. 126, 301–307.

Liu, C., Xu, X., Li, B., Situ, B., Pan, W., Hu, Y., An, T., Yao, S., Zheng, L., 2018. Single-exosome-counting immunoassays for cancer diagnostics. Nano Lett. 18 (7), 4226–4232.

Liu, C., Zhao, J., Tian, F., Cai, L., Zhang, W., Feng, Q., Chang, J., Wan, F., Yang, Y., Dai, B., 2019. Low-cost thermophoretic profiling of extracellular-vesicle surface proteins for the early detection and classification of cancers. Nat. Biomed. Eng. 3 (3), 183.

Miller, M., Sheehan, P., Edelstein, R., Tamanaha, C., Zhong, L., Bounnak, S., Whitman, L., Colton, R., 2001. A DNA array sensor utilizing magnetic microbeads and magnetoelectronic detection. J. Magn. Magn. Mater. 225 (1–2), 138–144.

Rife, J., Miller, M., Sheehan, P., Tamanaha, C., Tondra, M., Whitman, L., 2003. Design and performance of GMR sensors for the detection of magnetic microbeads in biosensors. Sens. Actuators A Phys. 107 (3), 209–218.

Schotter, J., Kamp, P.-B., Becker, A., Pühler, A., Reiss, G., Brückl, H., 2004. Comparison of a prototype magnetoresistive biosensor to standard fluorescent DNA detection. Biosens. Bioelectron. 19 (10), 1149–1156.

Shao, H., Chung, J., Lee, K., Balaj, L., Min, C., Carter, B.S., Hochberg, F.H., Breakefield, X.O., Lee, H., Weissleder, R., 2015. Chip-based analysis of exosomal mRNA mediating drug resistance in glioblastoma. Nat. Commun. 6, 6999.

Shao, H., Im, H., Castro, C.M., Breakefield, X., Weissleder, R., Lee, H., 2018. New technologies for analysis of extracellular vesicles. Chem. Rev. 118 (4), 1917–1950.

Sheridan, C., 2016. Exosome Cancer Diagnostic Reaches Market. Nature Publishing Group.

Su, S., Cao, W., Liu, W., Lu, Z., Zhu, D., Chao, J., Weng, L., Wang, L., Fan, C., Wang, L., 2017. Dual-mode electrochemical analysis of microRNA-21 using gold nanoparticle-decorated MoS2 nanosheet. Biosens. Bioelectron. 94, 552–559.

Su, S., Han, X., Lu, Z., Liu, W., Zhu, D., Chao, J., Fan, C., Wang, L., Song, S., Weng, L., 2017. Facile synthesis of a MoS2–Prussian blue nanocube nanohybrid-based electrochemical sensing platform for hydrogen peroxide and carcinoembryonic antigen detection. ACS Appl. Mater. Interfaces 9 (14), 12773–12781.

Sui, C., Li, F., Wu, H., Yin, H., Zhang, S., Waterhouse, G.I., Wang, J., Zhu, L., Ai, S., 2019. Photoelectrochemical biosensor for 5hmC detection based on the photocurrent inhibition effect of ZnO on MoS2/C3N4 heterojunction. Biosens. Bioelectron. 142, 111516.

Sun, X., Lei, C., Guo, L., Zhou, Y., 2016. Separable detecting of Escherichia coli O157H: H7 by a giant magneto-resistance-based bio-sensing system. Sens. Actuators B Chem. 234, 485–492.

Van Niel, G., D'Angelo, G., Raposo, G., 2018. Shedding light on the cell biology of extracellular vesicles. Nat. Rev. Mol. Cell Biol. 19 (4), 213.

Wang, M., Yin, H., Zhou, Y., Sui, C., Wang, Y., Meng, X., Waterhouse, G.I., Ai, S., 2019. Photoelectrochemical biosensor for microRNA detection based on a MoS2/g-C3N4/black TiO2 heterojunction with Histostar@ AuNPs for signal amplification. Biosens. Bioelectron. 128, 137–143.

Wang, W., Luo, J., Wang, S., 2018. Recent progress in isolation and detection of extracellular vesicles for cancer diagnostics. Adv. Healthc. Mater. 7 (20).

Xu, L., Yu, H., Akhras, M.S., Han, S.-J., Osterfeld, S., White, R.L., Pourmand, N., Wang, S. X., 2008. Giant magnetoresistive biochip for DNA detection and HPV genotyping. Biosens. Bioelectron. 24 (1), 99–103.

Yin, Z., Li, H., Li, H., Jiang, L., Shi, Y., Sun, Y., Lu, G., Zhang, Q., Chen, X., Zhang, H., 2011. Single-layer MoS2 phototransistors. ACS Nano 6 (1), 74–80.

Zhang, H., Chhowalla, M., Liu, Z., 2018. 2D nanomaterials: graphene and transition metal dichalcogenides. Chem. Soc. Rev. 47 (9), 3015–3017.

Zhang, H., Wang, Z., Zhang, Q., Wang, F., Liu, Y., 2019. Ti3C2 MXenes nanosheets catalyzed highly efficient electrogenerated chemiluminescence biosensor for the detection of exosomes. Biosens. Bioelectron. 124, 184–190.

Zhi, X., Deng, M., Yang, H., Gao, G., Wang, K., Fu, H., Zhang, Y., Chen, D., Cui, D., 2014. A novel HBV genotypes detecting system combined with microfluidic chip, loop-mediated isothermal amplification and GMR sensors. Biosens. Bioelectron. 54, 372–377.

Zhu, C., Zeng, Z., Li, H., Li, F., Fan, C., Zhang, H., 2013. Single-layer MoS2-based nanoprobes for homogeneous detection of biomolecules. J. Am. Chem. Soc. 135 (16), 5998–6001.